University of Zurich[UZH]

Zurich Open Repository and Archive
University of Zurich
University Library
Strickhofstrasse 39
CH-8057 Zurich
www.zora.uzh.ch

Year: 2016

HSAN1 mutations in serine palmitoyltransferase reveal a close structure-function-phenotype relationship

Bode, Heiko ; Bourquin, Florence ; Suriyanarayanan, Saranya ; Wei, Yu ; Alecu, Irina ; Othman, Alaa ; von Eckardstein, Arnold ; Hornemann, Thorsten

Abstract: Hereditary sensory and autonomic neuropathy type 1 (HSAN1) is a rare autosomal dominant inherited peripheral neuropathy caused by mutations in the SPTLC1 and SPTLC2 subunits of serine palmitoyltransferase (SPT). The mutations induce a permanent shift in the substrate preference from l-serine to l-alanine, which results in the pathological formation of atypical and neurotoxic 1-deoxy-sphingolipids (1-deoxySL). Here we compared the enzymatic properties of 11 SPTLC1 and six SPTLC2 mutants using a uniform isotope labelling approach. In total, eight SPT mutants (STPLC1p.C133W, p.C133Y, p.S331F, p.S331Y and SPTLC2p.A182P, p.G382V, p.S384F, p.I504F) were associated with increased 1-deoxySL synthesis. Despite earlier reports, canonical activity with l-serine was not reduced in any of the investigated SPT mutants. Three variants (SPTLC1p.S331F/Y and SPTLC2p.I505Y) showed an increased canonical activity and increased formation of C20 sphingoid bases. These three mutations are associated with an exceptionally severe HSAN1 phenotype, and increased C20 sphingosine levels were also confirmed in plasma of patients. A principal component analysis of the analysed sphingoid bases clustered the mutations into three separate entities. Each cluster was related to a distinct clinical outcome (no, mild and severe HSAN1 phenotype). A homology model based on the protein structure of the prokaryotic SPT recapitulated the same grouping on a structural level. Mutations associated with the mild form clustered around the active site, whereas mutations associated with the severe form were located on the surface of the protein. In conclusion, we showed that HSAN1 mutations in SPT have distinct biochemical properties, which allowed for the prediction of the clinical symptoms on the basis of the plasma sphingoid base profile.

DOI: https://doi.org/10.1093/hmg/ddv611

Posted at the Zurich Open Repository and Archive, University of Zurich
ZORA URL: https://doi.org/10.5167/uzh-120653
Journal Article
Published Version

Originally published at:
Bode, Heiko; Bourquin, Florence; Suriyanarayanan, Saranya; Wei, Yu; Alecu, Irina; Othman, Alaa; von Eckardstein, Arnold; Hornemann, Thorsten (2016). HSAN1 mutations in serine palmitoyltransferase reveal a close structure-function-phenotype relationship. Human Molecular Genetics, 25(5):853-865.
DOI: https://doi.org/10.1093/hmg/ddv611

OXFORD

Human Molecular Genetics, 2016, Vol. 25, No. 5 853–865

doi: 10.1093/hmg/ddv611
Advance Access Publication Date: 17 December 2015
Original Article

ORIGINAL ARTICLE

HSAN1 mutations in serine palmitoyltransferase reveal a close structure–function–phenotype relationship

Heiko Bode[1,2], Florence Bourquin[4], Saranya Suriyanarayanan[1,3], Yu Wei[1], Irina Alecu[1,2], Alaa Othman[1,3], Arnold Von Eckardstein[1,2,3] and Thorsten Hornemann[1,2,3,*]

[1]Institute for Clinical Chemistry, University Hospital Zurich, [2]Center for Integrative Human Physiology, University of Zurich, Zurich, Switzerland, [3]Competence Center for Personalized Medicine (CC-PM), Molecular Translation and Biomedicine (MTB), and [4]Institute of Biochemistry, University of Zurich, Zurich, Switzerland

*To whom correspondence should be addressed at: Institute for Clinical Chemistry, University Hospital Zurich, Raemistrasse 100, CH8091 Zurich, Switzerland. Tel: +41 442554719/+41 445563101; Fax: +41 442554590; Email: thorsten.hornemann@usz.ch

Abstract

Hereditary sensory and autonomic neuropathy type 1 (HSAN1) is a rare autosomal dominant inherited peripheral neuropathy caused by mutations in the SPTLC1 and SPTLC2 subunits of serine palmitoyltransferase (SPT). The mutations induce a permanent shift in the substrate preference from L-serine to L-alanine, which results in the pathological formation of atypical and neurotoxic 1-deoxy-sphingolipids (1-deoxySL). Here we compared the enzymatic properties of 11 SPTLC1 and six SPTLC2 mutants using a uniform isotope labelling approach. In total, eight SPT mutants (STPLC1p.C133W, p.C133Y, p.S331F, p.S331Y and SPTLC2p.A182P, p.G382V, p.S384F, p.I504F) were associated with increased 1-deoxySL synthesis. Despite earlier reports, canonical activity with L-serine was not reduced in any of the investigated SPT mutants. Three variants (SPTLC1p.S331F/Y and SPTLC2p.I505Y) showed an increased canonical activity and increased formation of C_{20} sphingoid bases. These three mutations are associated with an exceptionally severe HSAN1 phenotype, and increased C_{20} sphingosine levels were also confirmed in plasma of patients. A principal component analysis of the analysed sphingoid bases clustered the mutations into three separate entities. Each cluster was related to a distinct clinical outcome (no, mild and severe HSAN1 phenotype). A homology model based on the protein structure of the prokaryotic SPT recapitulated the same grouping on a structural level. Mutations associated with the mild form clustered around the active site, whereas mutations associated with the severe form were located on the surface of the protein. In conclusion, we showed that HSAN1 mutations in SPT have distinct biochemical properties, which allowed for the prediction of the clinical symptoms on the basis of the plasma sphingoid base profile.

Introduction

Hereditary sensory and autonomic neuropathies (HSANs) represent a group of neurologic disorders with high genotypic and phenotypic variability that affect the peripheral nervous system. HSANs have been subdivided into seven classes with distinct phenotypes (1–3). HSAN type 1 (HSAN1) differs from the other forms (HSAN2–7) by its autosomal dominant inheritance (2,4). It is a mutilating, axonal neuropathy typically characterized by a slow and progressive sensory loss and the formation of perforating ulcers at the feet and hands. Typically, first clinical symptoms appear between the second and fifth decade (1,4,5). Pathological features include atrophy and demyelination in the cauda equine and thinning of the sciatic and ulnar nerves, atrophy of the dorsal root ganglia and significant loss of myelinated fibres in several afferent peripheral nerves (6).

Received: October 21, 2015. **Revised and Accepted:** December 12, 2015

© The Author 2015. Published by Oxford University Press. All rights reserved. For Permissions, please email: journals.permissions@oup.com

HSAN1 has been associated with mutations in six genes: *SPTLC1* (7,8), *SPTLC2* (9), *ATL1* (10), *DNMT1* (11), *RAB7* (12) and *ATL3* (13). The majority of the identified HSAN1 patients carry mutations in *SPTLC1* or *SPTLC2*. These genes encode for two out of three core subunits of the serine palmitoyltransferase (SPT). SPT is a pyridoxal phosphate (PLP)-dependent α-oxoamine synthase (POAS), which catalyses the condensation of palmitoyl-CoA and L-serine, the first and rate limiting step in the de novo synthesis of sphingolipids. Mammalian SPT is a heteromeric complex consisting of the ubiquitously expressed subunits SPTLC1 and SPTLC2 and the more tissue-specific SPTLC3. All three subunits show a similarity on the amino acid level (14), but only SPTLC2 and SPTLC3 contain a PLP binding motif. The three SPT subunits interact in a tissue-specific manner and probably form a hetero-octameric structure consisting of four active dimers (15).

Initially, the HSAN1 locus was mapped to chromosome 9q22.1–q22.3 (16) and subsequently, three point mutations in the *SPTLC1* gene (p.C133W, p.C133Y and p.V144D) were found to be disease-causing (7,8). Later, four more SPTLC1 mutations (p.C133R, p.A352V, p.S331F and p.S331Y) (17–19) and mutations in SPTLC2 were reported to be disease-causing (p.A182P, p.G382V, p. V359M, p.S384F p.T409M and p.I504F) (20). Other mutations have also been reported, but not conclusively linked to the disease yet. An SPTLC1p.G387A variant was initially believed to cause a severe form of HSAN1, but was later demonstrated not to be disease-causing (21,22). An SPTLC1p.R239W variant was found in a large breast cancer screen (23), and an inactivating mutation (SPTLC1p.G246R) was identified in an SPT activity-deficient CHO cell line (24,25). Furthermore, an SPTLC1p.R151L variant was annotated as a non-disease-causing polymorphism in a HSAN1 patient with a mutation in the small GTPase RAB7 (26), and an SPTLC1p.A339V mutation was identified in a German family with several affected individuals but showed an incomplete segregation pattern (unpublished data). An SPTLC2p.T409M mutant was identified in an isolated patient, but no other information about this patient was available to us.

Typically, HSAN1 mutations cause a permanent shift in the substrate preference of SPT resulting in the use of the non-canonical amino acid substrates L-alanine and glycine, thereby forming the two atypical sphingoid bases 1-deoxy-sphinganine (1-deoxySA) and 1-deoxymethyl-sphinganine (1-doxmethSA) (27). Both metabolites lack the C_1 hydroxyl group of regular sphingoid bases, which precludes their metabolism to complex sphingolipids such as sphingomyelins, hexosylceramides or gangliosides. The missing OH-group also hampers their degradation by the canonical catabolic pathway, as this requires phosphorylation at C_1 to form the catabolic intermediate sphingosine-1-phosphate (27). Pathologically increased 1-deoxy-sphingolipid (1-deoxySL) levels were found in plasma and lymphoblasts of HSAN1 patients (27,28), representing a biochemical hallmark of HSAN1 but also a reliable biomarker for diagnosis.

1-DeoxySLs are toxic to a variety of cell lines (29–32). Neurotoxicity was demonstrated in cultured primary chicken neurons (27,33) and also reported from clinical phase I cancer studies, in which 1-deoxySA was tested as a novel, experimental anti-cancer drug (34,35). 1-DeoxySA-induced cell death was shown to be associated with cytoskeletal changes and the disassembly of actin stress fibres, indicating that a deregulation of cytoskeletal structures could be an underlying pathomechanism in HSAN1 (30). In fact, 1-deoxySLs were shown to alter cytoskeletal structures by activating the Rho–Rac pathways in β-cells (36).

Mirroring its genotypic variability, HSAN1 is also characterized by phenotypic variability. Certain SPT mutants, like SPTLC1p. V144D, were reported to be associated with rather mild symptoms, whereas some other variants (SPTLC1p.S331F and p.S331Y and SPTLC2p.I504F) cause a severe and early onset phenotype with anhydrosis, prominent muscle atrophy, growth retardation, ocular manifestations and lung complications (17,19,37,38).

In this study, we compared the enzymatic properties of 17 reported SPT mutants with the aim to provide a comprehensive characterization of these mutants and to see whether there is a correlation between the enzymatic feature of the mutants and the variability in the HSAN1 phenotypes.

Results

HSAN1 mutations do not reduce canonical SPT activity

In this study, we compared the enzymatic and biochemical properties of 17 SPT mutants (Fig. 1) in terms of activity and product spectrum. An overview of the analysed mutations and their associated clinical phenotypes is summarized in Table 1. All constructs were expressed in HEK293 cells, and expression was confirmed by western blot. SPT activity was analysed in living cells using a metabolic labelling assay. For labelling, cells were cultured for 24 h in the presence of isotope-labelled d3-N^{15}-L-serine (1 mM) and d4-L-alanine (2 mM) in serine- and alanine-free DMEM medium. This results in d3-labelled sphingoid bases, as one deuterium is exchanged with a hydrogen during condensation with palmitoyl-CoA. The total amount of de novo-formed sphingoid bases was analysed after removing the conjugated N-acyl chains and head groups by acid hydrolysis. In total, 17 sphingoid bases including C_{18}SA, C_{18}SO, 1-deoxySA, 1-deoxySO, C_{20}SA and C_{20}SO were quantified by LC–MS.

The overexpression of wild-type SPTLC1 did not increase SPT activity compared with controls (empty vector), whereas overexpressing SPTLC2 resulted in a 2-fold increase in SPT activity (Fig. 2A). Although reduced *in vitro* activity was reported previously for several of the mutants (39–48), none of the SPTLC1 and SPTLC2 mutants showed a reduced incorporation of d3-N^{15}-L-serine in our conditions. On the contrary, two SPTLC1 mutants (p.S331F and p.S331Y) and one SPTLC2 mutant (p.I504F) showed a significantly increased canonical activity. The 1-deoxySL formation in SPTLC1wt and SPTLC2wt overexpressing cells was comparable to controls (Fig. 2B), indicating that the wild-type SPT does not utilize significant amounts of L-alanine under these conditions. In contrast, several but not all SPT mutants showed an increased 1-deoxySL formation. Significantly increased 1-deoxySL levels were seen in cells expressing the mutants STPLC1p.C133W, p.C133Y, p.S331F, p.S331Y or SPTLC2p.A182P, p.G382V, p.S384F and p.I504F. In contrast, the SPTLC1 variants p.V144D, p.G246R, p.A339V and p.A352V and SPTLC2p.V359M and p.T409M did not show significant activity with d4-L-alanine.

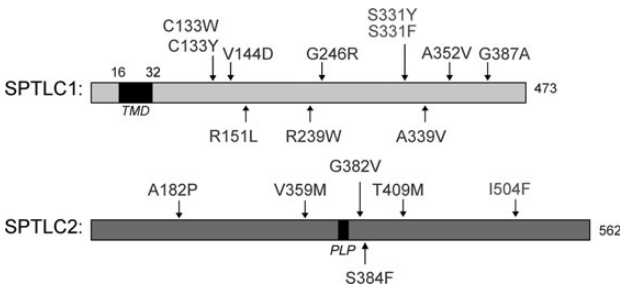

Figure 1. Overview of the 17 SPTLC1 and SPTLC2 mutations analysed.

Table 1. Overview of clinical features of HSAN1 patients with SPTLC1 mutations [combined and adapted from (9,17,38)]

Mutation	Origin/ inheritance	AAO (years)	Type of polyneuropathy	Weakness	Ulcers/ amputation	Respiratory problems	Cataracts (age)	Other symptoms	Reference
SPTLC1p.C133W	Australian English/NM	65	NM	Yes in 4/38	Yes	NM	NM	NS	Dawkins *et al.* (8)
SPTLC1p.C133W	Canadian/NM	20–40	NM	Yes in 6/7	Yes	NM	NM	NS	Bejaoui *et al.* (7)
SPTLC1p.C133W	Chinese/AD	20s	Sensory motor	No	Yes	NM	NM	NS	Bi *et al.* (63)
SPTLC1p.C133W	Canadian/AD	12, 60s	Sensory	Peroneal atrophy	Yes	NM	NM	NS	Klein *et al.* (64)
SPTLC1p.C133W	English/AD and IC	12–70, Avg = 29	Sensory motor	Yes	Yes	NM	NM	NS	Houlden *et al.* (5)
SPTLC1p.C133Y	German/NM	NM	NM	NM	NM	NM	NM	NS	Bejaoui *et al.* (7)
SPTLC1p.C133Y	Australian German/NM	NM	NM	NM	NM	NM	NM	NS	Dawkins *et al.* (8)
SPTLC1p.C133Y	Portuguese/AD	20s, 10	Sensory motor	No	No	NM	No	Foot pain, dry skin	Geraldes *et al.* (65)
SPTLC1p.C133R	German/AD	50	None	No	NM	NM	NM	NS	Rautenstrauss *et al.*
SPTLC1p.V144D	Australian German/NM	NM	NM	NM	NM	NM	NM	NS	Dawkins *et al.* (8)
SPTLC1p.A310G	English/IC	50s	Sensory	No	Yes	NM	NM	NS	Davidson *et al.* (66)
SPTLC1p.S331F	German/IC	Early childhood	Sensory motor	Yes	Yes	NM	Yes (9)	Sweating disturbances and anhydrosis, joint contractures, fractures	Huehne *et al.* (37)
SPTLC1p.S331F	French (Gypsy)/IC	Congenital	Sensory motor	Yes	Yes	Yes	Yes	Joint hyperlaxity, severe growth and mental retardation, microcephaly, hypotonia, vocal cord paralysis, gastro-oesophagial reflux	Rotthier *et al.* (19)
	Korean/IC	5	Sensory motor	Yes walker (27)a	Yes	Yes	Yes (10)	Hoarseness, tremor, scoliosis	Suh *et al.* (38)
SPTLC1p.S331Y	Austria/IC	4	Sensory motor	Yes wheelchair (14) a	Yes	Yes	Yes (13)	Tremor, fasciculation, joint hypermobility, pes cavus	Auer-Grumbach *et al.* (17)
SPTLC1p.A352V	Austrian/IC	16	Sensory motor	Distal LL, peroneal atrophy	No	NM	NM	Mild pes cavus, lancinating pains	Rotthier *et al.* (19)
SPTLC2 p.V359M	Austrian/IC	52 years	Axonal/intermediatesensory motor	NM	Yes/greatR toe	NM	NM	Ulceration and amputation of great R toe	Rotthier *et al.* (9)
SPTLC2 p.G382V	German/D	37 years	Axonal/intermediatesensory motor	Yes UL and LL	No	NM	NM	Dysesthesia and sensory loss distal UL and LL	Rotthier *et al.* (9)
SPTLC2 p.G382V	Austrian/D	38 years, mother asymptomatic	Axonal sensory motor	Yes LL	No	NM	NM	Sensory loss in feet	Rotthier *et al.* (9)
SPTLC2p.I504F	Czech/IC(de novo)	5 years	Intermediate sensory motor	Yes (LL)	Yes (LL)	NM	NM	Sweating disturbances and anhydrosis, gait difficulties, foot deformities	Rotthier *et al.* (9)

AAO, age at onset; PN, polyneuropathy; IC, isolated case; SM, sensory motor polyneuropathy; NM, not mentioned; AD, autosomal dominant; IC, isolated case; LL, lower limbs; UL, upper limbs; NS, not specified.

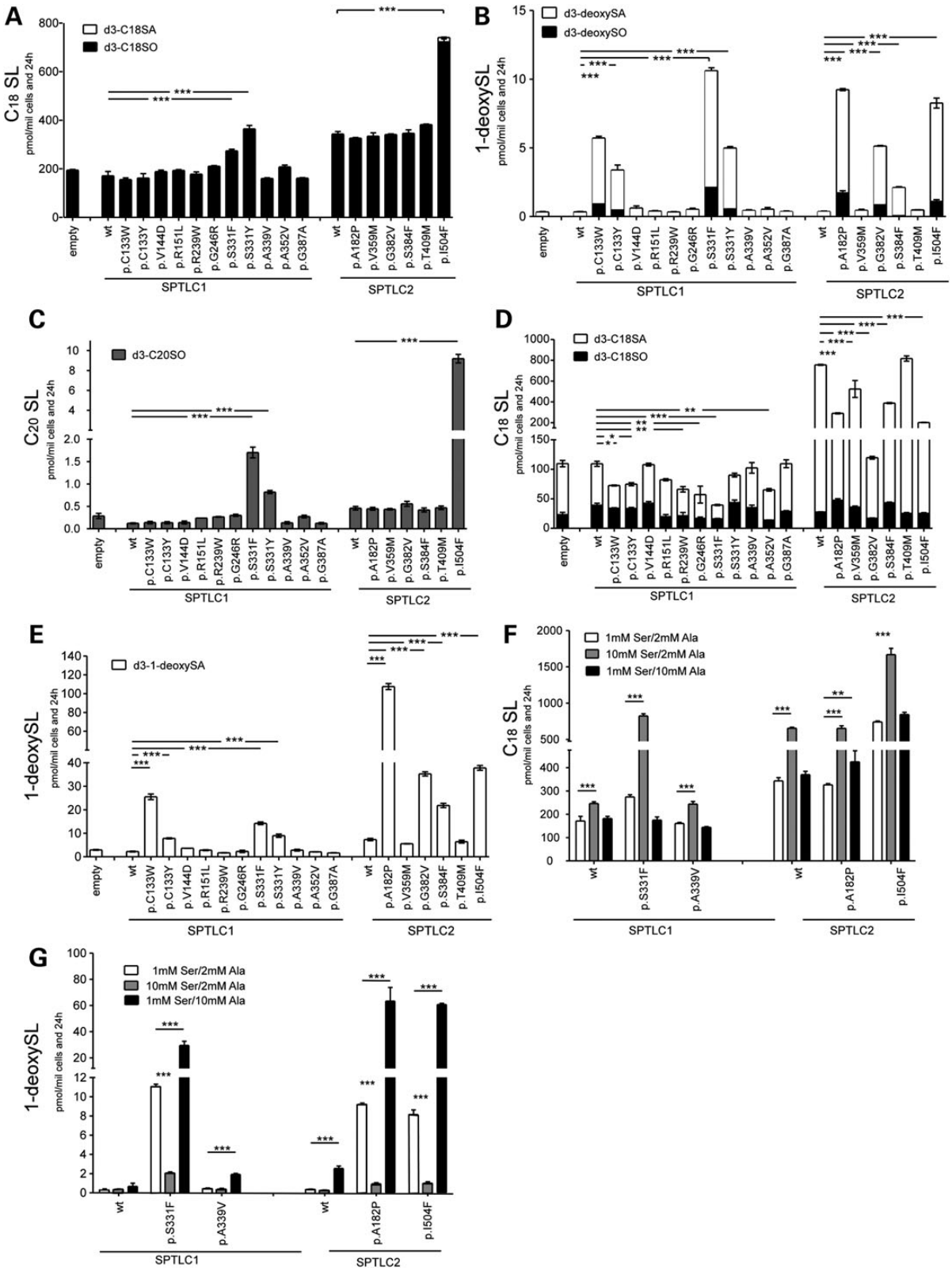

Figure 2. De novo formation of C_{18} sphinganine (d3-C18SA) and C_{18} sphingosine (d3-C18SO) (**A**); 1-deoxySA (d3-deoxySA) and 1-deoxySO (d3-deoxySO) (**B**) and C_{20} sphingosine (d3-C20SO) (**C**) in mutant-expressing HEK293 cells within 24 h. De novo formation of C_{18} sphinganine (d3-C18SA) and C_{18} sphingosine (d3-C18SO) (**D**) and of 1-deoxySA (d3-deoxySA) and 1-deoxySO (d3-deoxySO) (**E**) in the presence of Fumonisin B1 (35 μM). Cells were transfected with the empty vector (empty), SPTLC1wt, SPTLC2wt or the individual HSAN1 mutations and cultured in the presence of d3-N_{15}-L-serine (1 mM) and d4-L-alanine (2 mM), respectively. De novo formation of canonical SLs (**F**) and 1-deoxySLs (**G**) in relation to the availability of serine and alanine. HEK293 cells expressing the SPTLC1wt, p.S331F, p.A339V or SPTLC2wt, p. A182P, I504F were cultured for 24 h at different concentrations of d3-L-serine and d4-L-alanine (1 mM Ser/2 mM Ala, 10 mM Ser/2 mM Ala and 1 mM Ser/10 mM Ala). Labelled sphingoid bases were quantified by LC–MS after hydrolysis. Statistical significance was calculated by one-way ANOVA followed by Dunnett's multiple comparison test. $^{*}P < 0.01$; $^{**}P < 0.001$ and $^{***}P < 0.0001$.

Besides palmitoyl-CoA, SPT can also use other acyl-CoAs in the range of C14–C18, thereby forming sphingoid bases with different carbon chain lengths. Comparing the mutants for their ability to form sphingoid bases other than C_{18}, we observed significantly increased C_{20} sphingoid base levels in cells expressing the mutants SPTLC1p.S331F, p.S331Y and SPTLC2p.I504F (Fig. 2C). C_{20} sphingoid bases are formed by the conjugation of stearyl-CoA and L-serine, and increased levels of these sphingoid bases have not yet reported in the context of HSAN1. An increased C_{20} sphingoid base formation was only seen for this particular subclass of HSAN1 mutants.

Interestingly, the activity pattern of the mutants changed in the presence of the mycotoxin Fumonisin B1 (FB1), a potent inhibitor of ceramide synthase (CerS). CerS catalyses the acylation of sphinganine to dihydroceramide: the subsequent step in the de novo synthesis pathway. Blocking CerS by FB1 led to an accumulation of the precursor sphinganine (42) and was reported previously to increase 1-deoxySA formation in cells (29). The addition of FB1 induced significant changes in the canonical activity of the mutants. Although SPT activity in SPTLC1p.V144D, p.A339V and p.G387A expressing cells was comparable to controls, cells expressing the mutants SPTLC1p.C133W, p.C133Y, p.R239W, p.G246R and p.A352V showed a significantly reduced activity in the presence of FB1 (Fig. 2D). The activity of SPTLC2p.A182P, p.V359M, p.G382V and p.S384F was also reduced compared with wild-type SPTLC2, whereas the activity of SPTLC2p.T409M was not altered. Interestingly, those mutations which initially had an increased canonical activity (SPTLC1p.S331Y/F and SPTLC2p.I505F) showed a more pronounced reduction in activity in the presence of FB1. In contrast, the pattern of 1-deoxySL formation was not changed in the presence of FB1 (Fig. 2E). However, certain mutants showed a several fold increase in 1-deoxySL levels in the presence of FB1. For SPTLC1p.C133W and p.C133Y, 1-deoxySL formation increased 4.5- and 2.3-fold, respectively, whereas this effect was less pronounced for SPTLC1p.S331F and p.S331Y (1.3- and 1.8-fold, respectively). SPTLC2p.I504F and p.A182P showed a 4- and 10-fold increase in 1-deoxySL formation, respectively.

The formation of 1-deoxySLs is modulated by the availability of L-serine and L-alanine (43). 1-DeoxySL formation was effectively suppressed in a HSAN1 mouse model by L-serine-enriched food, which was shown to protect the animals from developing neurological symptoms (43). A significant reduction of plasma 1-deoxySL levels was also observed in HSAN1 patients who received oral supplementation with L-serine in the context of a clinical pilot trial (43). In contrast, increased availability of L-alanine resulted in augmented 1-deoxySL formation and aggravated neuropathic symptoms in the HSAN1 mouse model (43). We therefore compared the effect of L-serine and L-alanine on a set of selected mutants (Fig. 2F and G). At 10 mM L-serine, we observed a slightly increased canonical activity in all cells, although this increase was significantly more pronounced in cell expressing the p.S331F mutant (Fig. 2F). In parallel, 1-deoxySL formation was greatly suppressed at elevated L-serine levels, whereas 10 mM alanine significantly stimulated 1-deoxySL formation in all mutant-expressing cells (Fig. 2G). No significant increase in 1-deoxySL formation was seen in SPTLC1wt and SPTLC2wt overexpressing cells in the presence of 10 mM alanine. Except for a slight stimulatory effect in SPTLC2p.A182P expressing cells, L-alanine had no significant influence on the canonical activity of SPT.

Activity of HSAN1 mutants in LYB cells

All previous experiments were performed in HEK293 cells on the background of the endogenously expressed wild-type SPT. Although this mirrors the dominant trait in HSAN1, it does not allow for analysing the residual activity of the mutants. We therefore tested the mutants in LYB cells, a CHO cell line that is deficient in endogenous SPT activity due to a spontaneous mutation in the SPTLC1 subunit. The mutation was subsequently identified as SPTLC1p.G246R. Expressing a functional wild-type SPTLC1 is sufficient to restore SPT activity in these cells (24,25). We used LYB cells to compare the activity of SPTLC1wt, p.C133W, pG246R, S331F in the presence and absence of FB1 (Fig. 3). As controls, we also expressed SPTLC2wt and p.I504F in these cells, although it is not expected that this results in a recovery of enzyme activity, as the underlying mutation is located in the SPTLC1 subunit. Accordingly, the expression of wild-type SPTLC1 but not of SPTLC2 restored activity (Fig. 3). Expressing the mutant p.C133W restored canonical activity only marginally, and activity was further reduced in the presence of FB1.

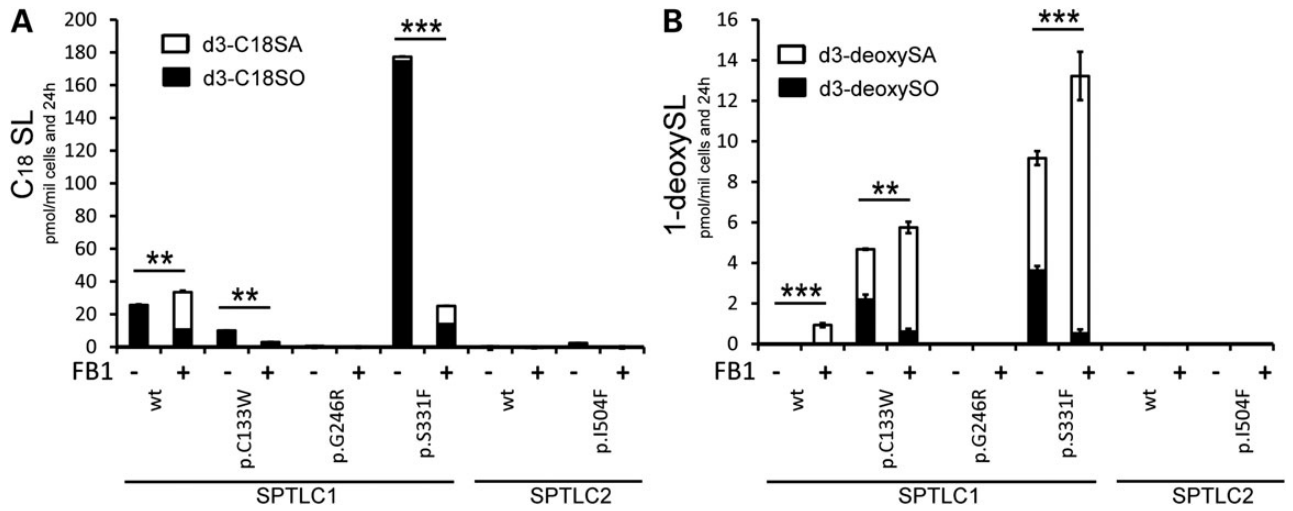

Figure 3. De novo formation of (**A**) C_{18} sphinganine (d3-C18SA) and C_{18} sphingosine (d3-C18SO) and (**B**) 1-deoxySA (d3-deoxySA) and 1-deoxySO (d3-deoxySO) in mutant-expressing LYB cells. Activity was tested in the presence and absence of Fumonisin B1. Labelled sphingoid bases were quantified by LC–MS after hydrolysis. **P < 0.001 and ***P < 0.0001.

Interestingly, the capacity to form 1-deoxySLs remained intact in this mutant, indicating that the mutation primarily affects the activity with L-serine. As expected, expression of p.G246R, which is the same mutation that is present in LYB endogenously, neither restored canonical activity nor resulted in the formation of 1-deoxySL. In contrast, expression of the p.S331F mutant fully restored canonical activity, and activity was even 9–10-fold higher compared with the wild-type subunit. Activity with alanine was also present, and 1-deoxySL formation was about 2-fold higher compared with p.C133W cells. However, in the presence of FB1, canonical activity of p.S331F dropped greatly, whereas 1-deoxySL formation was increased by 30%. Similar to the expression of the wild-type SPTLC2, the expression of p.I504F was not able to restore activity in LYB cells.

Genotype–phenotype association in HSAN1

To further stratify the biochemical properties of the tested mutants, we performed a PCA for all 20 constructs (17 mutants, two wild-type subunits and control cells). As variables, we included the ratios (mut:wt) for de novo-formed d3-C_{17}SO; d3-sphingadiene; d3-C_{18}SA; d3-C_{18}SO; d3-C_{20}SO; d3-deoxySA and d3-deoxySO. This generated two principal components that separated the mutants into three isolated clusters (Fig. 4A). As expected, the assigned discriminatory weight for the suggested model identified the two 1-deoxySL species and C_{20}SO as the strongest discriminators for the clustering (Fig. 4B). Strikingly, the three clusters perfectly mirrored the associated clinical HSAN1 phenotypes. The first group comprised all mutations that showed no change in the canonical activity (in the absence of FB1). In the metabolic labelling assay, these variants behaved similar to the respective wild-type subunits and did not form increased levels of 1-deoxySLs nor C_{20}-sphingoid bases. This cluster is not associated with a disease phenotype.

The second cluster included mutations that were associated with increased 1-deoxySL formation but an unaltered canonical activity. This group comprised the mutations SPTLC1p.C133W and p.C133Y and SPTLC2p.A182P, p.G382V and p.S384F. These mutations are associated with a typical late-onset HSAN1 phenotype, with primarily sensory and mild motor impairments. Within this cluster, the SPTLC1p.C133Y and p.C133W are the most frequently found mutations in HSAN1 and appear in several large kinships in Europe, USA and Australia. Also the three SPTLC2 mutations p.G382V, p.S384F and p.A182P were reported to be associated with a rather typical HSAN1 phenotype.

The third cluster consisted of three mutants (SPTLC1p.S331F, p.S331Y and SPTLC2p.I504F). This group was characterized by an increased formation of C_{18}-, 1-deoxy- and C_{20}-sphingoid bases. In particular, the increased formation of C_{20}-based sphingolipids is a unique hallmark of this group. These three mutations are

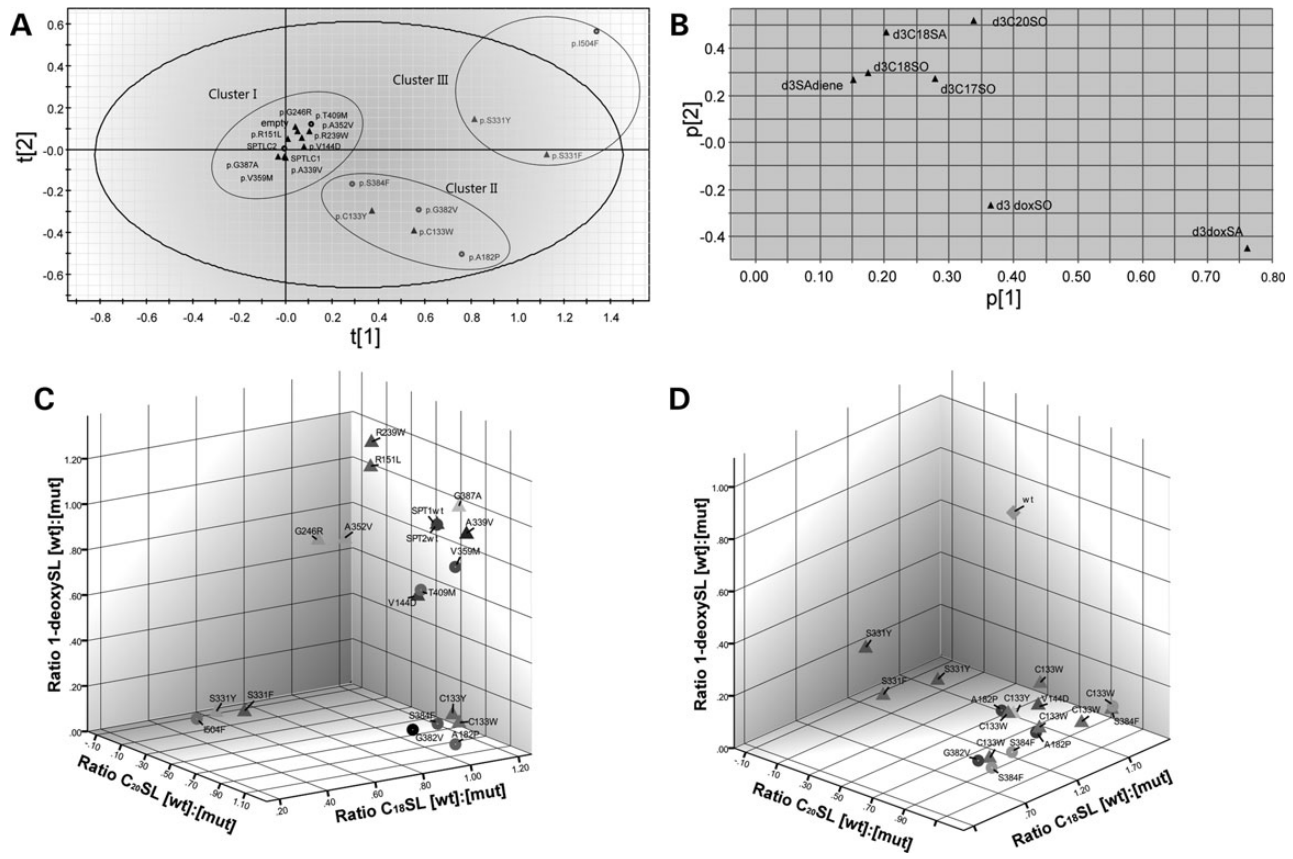

Figure 4. (**A**) Score scatter plot of a PCA based on the ratios mut:wt for C_{17}SO, SAdiene, C_{18}SA, C_{18}SO, C_{20}SO, 1-deoxySA and 1-deoxySO; R2X[1] = 0.79, R2X[2] = 0.15. (**B**) Loading scatter plot of the PCA. Distance and direction from the origin of the axes equal the assigned weight and importance of the individual sphingolipid species for the grouping of the mutants. (**C**) Clustering of the different HSAN1 mutations based on their activity in forming C_{18}SL, C_{20}SL and 1-deoxySL. Shown are the ratios (wt:mutant) of de novo formed (deoxy)sphingoid bases in mutant-expressing HEK293 cells, which were cultured for 24 h in the presence of d3-N_{15}1-L-serine (1 mM) and d4-L-alanine (2 mM). (**D**) Clustering of the different HSAN1 mutations based on the levels for C_{18}SL, C_{20}SL and 1-deoxySL in plasma samples from patients. The figure is based on previously published plasma data from HSAN1 patients (9,17,20,27,44,45). The depicted numbers reflect the underlying mutation (triangle, SPTLC1; circle, SPTLC2). Identical numbers reflect the same mutation from different patients.

associated with an exceptionally severe HSAN1 phenotype characterized by early or even congenital onset, growth retardation, autonomic impairments (sweating), motor neuron defects, juvenile cataracts and weakness in the respiratory system. Plotting the ratios of C_{18} SO, 1-deoxySL and C_{20}SL in the individual mutants relative to the wild-type subunit resulted in a similar clustering as seen in the PCA (Fig. 4C). A similar clustering was observed when analysing the sphingoid bases in plasma samples from HSAN1 patients (Fig. 4D). Unfortunately, plasma samples were only available for seven out of the 17 analysed mutations. No difference in canonical C_{18} sphingoid bases was seen in any of the analysed plasma samples. Mirroring the results from the cell culture experiments, SPTLC1p.C133W, p.C133Y and p.V144D carriers presented with elevated 1-deoxySL levels and unchanged C_{20}SL levels. In line with the cell culture experiments, we observed elevated 1-deoxySL and C_{20}-sphingoid bases in plasma from p.S331Y/F carriers. Plasma from an I505F carrier was not available. The plasma of an SPTLC1p.R151L carrier which was analyzed here for the first time did not show increased 1-deoxySL, C18SL or C20SL levels, indicating that this mutation is not disease-associated.

Structure–function relationship

In continuation of the biochemical analysis, we wanted to see whether the biochemical features of the different HSAN1 mutants can be mapped onto specific regions of the protein. To this purpose, we generated a homology model for the human SPT dimer based on the prokaryotic SPT structure from *S. paucimobilis* (PBD entry code 2JG2). Similar to the functional analysis, the structural analysis also assigned the mutants into three distinct groups. The first group comprised all mutants that could not be assigned to any specific structural cluster (Fig. 5A). This first group did not show altered SPT activity nor significant 1-deoxySL formation and corresponds to the central cluster 1 in Figure 4A. Most amino acid exchanges within this group are conservative, and the expected structural impact for these mutations is minor except for SPTLC2p.T409, which is prominently located at the interface between SPTLC1 and SPTLC2. However, whether an exchange from T to the more polar M has an impact on the interaction of the subunits is difficult to assess. The second group comprised the residues SPTLC1p.C133, SPTLC2p.A182, p.G382 and p.S384, which are all located around the internal aldimine in SPTLC2 (Fig. 4B). This group corresponds to cluster 2 in Figure 4A and is associated with normal canonical activity but increased 1-deoxySL formation. Residue p.C133 is part of SPTLC1 which by itself does not bear a PLP binding site, but is located close to the internal aldimine of the SPTLC2 subunit. A change to W and Y is expected to have an impact on activity, probably by modifying the binding properties of the incoming substrates. The mutant SPTLC2p.A182P might alter the flexibility of the PLP region, having also a significant impact on the binding of the substrates. The SPTLC2p.S384F mutation is likewise supposed to alter the activity of the protein. The impact of the SPTLC2p.G382V mutation is more difficult to estimate, as the exchange from G to V conserves the physicochemical properties of the residue. However, this replacement may influence the dynamics of the loops surrounding the active site. Except for the SPTLC1p.A339V, all these variants were associated with reduced canonical activity in the presence of FB1. On the basis of the position, the A339V mutation could also be assigned to cluster 2, but was functionally classified into cluster 1 as it was not associated with increased 1-deoxySL formation. The third group comprised two residues exposed at the surface of the protein, SPTLC1p.S331 and SPTLC2p.I504 (Fig. 5C). Mutations in the residues S331 and I504 were grouped into cluster 3 (Fig. 3A) and are associated with increased canonical activity as well as with increased 1-deoxySL and C_{20}SO formation. Residues R151 and V144 are also located on a surface-exposed helix (Fig. 4C, light blue), following the active site loop carrying C133. However, functionally residues R151 and V144 do not cluster into group 3 as they are clearly not associated with the same severe features as seen for S331F/Y and I504F. Indeed, both mutants did not show significantly altered activities in our analysis, although V144A was reported repeatedly to be associated with HSAN1.

Discussion

Here we compared 17 SPT mutants for their enzymatic activity and substrate affinity. The majority of the analysed variants were identified in patients with HSAN1. Using a metabolic labelling approach, we analysed SPT activity and product spectrum in an intact cellular context.

None of the analysed mutants showed a reduced formation of canonical C_{18} sphingoid bases, indicating that HSAN1 is not caused by a loss of activity as initially proposed (39,40,46). In contrast, three mutants showed an increased ability to form canonical C_{18}—as well as atypical C_{20} sphingoid bases (Fig. 2C). Elevated C_{20} sphingoid bases were also found in the plasma of patients with these mutations (Fig. 4C). Most HSAN1 mutants showed a significantly increased activity with alanine, leading to increased 1-deoxySL formation. However, two reported mutations in SPTLC1 (p.A339V and p.A352V) and SPTLC2 (p.T409M and p.V359M) did not match this pattern. SPTLC1p.A352V and SPTLC2p.V359M were already suggested previously not to be disease-causing (9,19), whereas SPTLC1p.A339V and SPTLC2p.T409M were not yet characterized. The SPTLC1p.A339V variant was found in a German patient who suffered from idiopathic neuropathy, but further sequencing of affected and non-affected family members revealed an incomplete segregation of this mutation within the family. For the SPTLC2p.T409M carrier, no clinical information was available. Both mutants seem to be benign as neither was associated with altered canonical activity nor significantly increased 1-deoxySL formation, although SPTLC1p.A339V showed slightly increased 1-deoxySL formation under high alanine conditions (Fig. 2G).

Surprisingly, the CerS inhibitor FB1 showed significant effects on the activity of some but not all mutants, although FB1 does not directly affect SPT activity. Several mutants (SPTLC1p.C133W, p.R151L, p.R239W, p.G243R, p.S331F, p.A352V and SPTLC2p.G382F) had a reduced canonical activity in the presence of FB1. This FB1-dependent change in canonical activity was most obvious in SPTLC1p.S331F-expressing LYB cells (Fig. 3A). In the presence of FB1, the activity pattern of the mutants generally resembled the pattern reported from cell-free *in vitro* assays. A reduced *in vitro* activity was previously reported for several of these mutants (39,40,46). Except for p.S331F/Y, most of the FB1-sensitive mutations are located in a cluster around the PLP binding site (Fig. 5B). Surprisingly, the ability to form 1-deoxySLs did not change in the presence of FB1. However, for some mutants, absolute 1-deoxySL levels were up to 10-fold higher in the presence of FB1, which is supported by earlier reports showing that FB1 stimulates the formation of 1-deoxySLs even in wild-type SPT (29). Expression of the mutants in LYB cells indicates that the activity with L-serine and L-alanine is independent and not directly linked. In general, we did not see a significant correlation between the formation of canonical SLs and 1-deoxySLs,

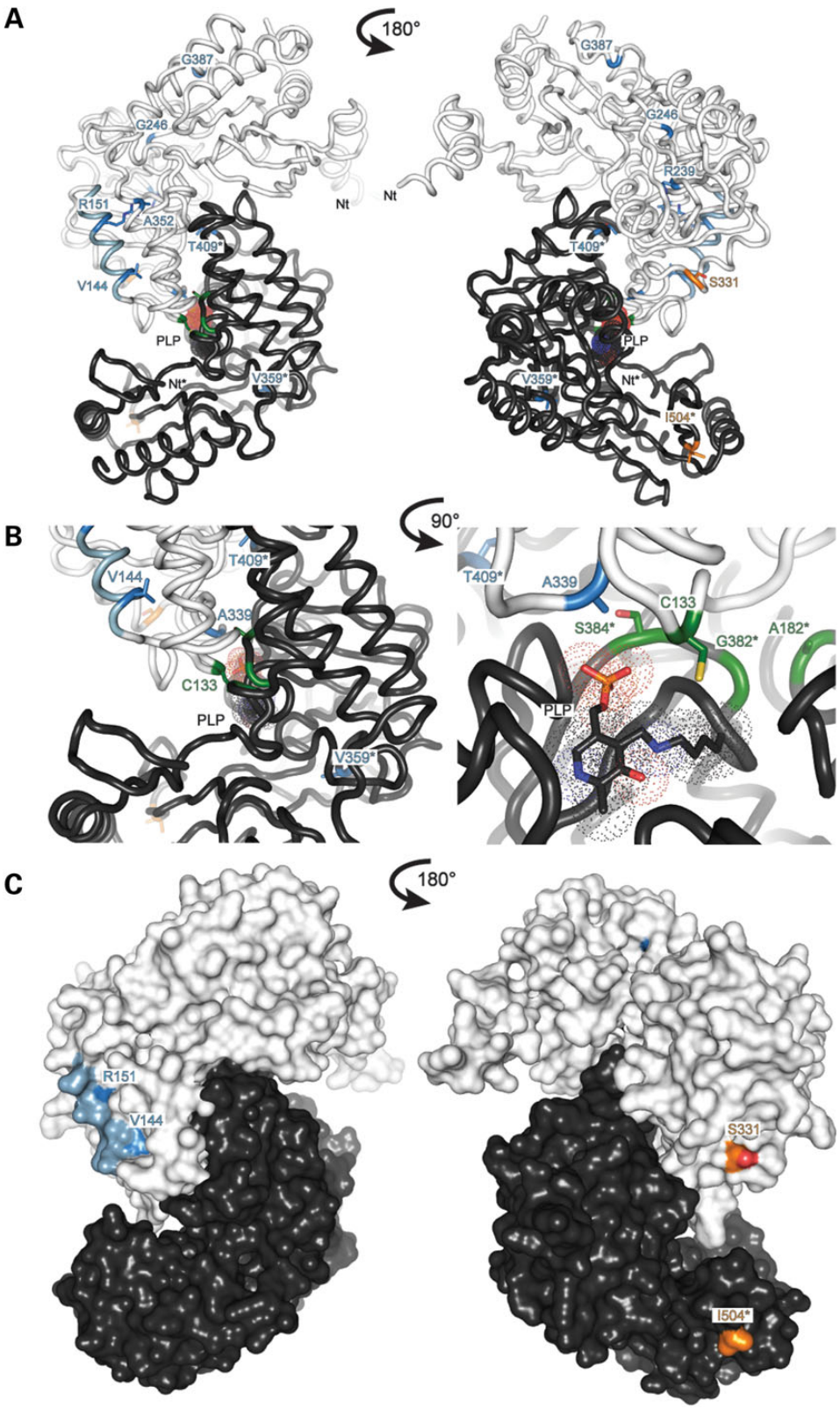

Figure 5. Homology model of the human SPTLC1-SPTLC2 dimer, coloured white and dark grey, respectively. (**A**) The mutations analysed in this work are depicted. The residues belonging to SPTLC2 are marked with an asterisk. The colour code is identical to Figure 4A. (**B**) Most of the mutations associated with a typical HSAN1 phenotype are located at the monomer–monomer interface and cluster around the PLP binding domain. (**C**) The two residues SPTLC1p.S331 and SPTLC2 p.I504F are located far away from the PLP binding site on the surface of the protein. Mutations in these residues are associated with a severe phenotype. All figures were prepared with Pymol. Mutations located in the SPTLC2 subunit are depicted with an asterisk.

neither in mutant-expressing cells nor in patient plasma. This shows discordance between canonical SPT activity and 1-deoxSL formation, meaning that the use of 1-deoxySLs as surrogate markers for SPT activity can lead to inappropriate interpretation of the canonical activity (47).

The observed differences in the presence of FB1 might be caused by a disturbance of the cellular mechanisms that regulate SL de novo synthesis. SPT activity seems to be tightly controlled by a metabolic feedback mechanism that counteracts the potentially harmful overproduction of ceramides. In yeast, this process is well understood and includes accessory proteins such as Orm1/2, Sac1 and Tsc3, which form a higher order complex called SPOTS (SPT, Orm1/2, Tsc3 and Sac1) (48). At sufficient SL levels, Orm1/2 associates with the complex and inhibits SPT activity. Upon SL shortage, Orm1/2 becomes gradually phosphorylated by Ypk1 kinase and, together with Sac1, dissociates from the complex, thereby releasing inhibition (48,49). Once SL levels are restored, Orm proteins get dephosphorylated again. As FB1 blocks the formation of products downstream of SA, this regulatory control might be eluded. However, it is unclear to which extent the same mechanism applies to higher eukaryotes. Mammalian cells express three ORM orthologues (ORMDL1–3) (50), but the Orm1/2 phosphorylation sites identified in yeast are not conserved. Individual or simultaneous overexpression of the ORMDL proteins has no effect on SPT activity, whereas the parallel silencing of all three but not of the individual ORMDL isoforms was reported to increase SPT activity (51). Furthermore, two small proteins (ssSPTa and ssSPTb) were identified in mammalian cells as functional orthologues of the yeast Tsc3 (52). Co-expression of the SPT core subunits SPTLC1 and 2 together with ssSPTa or ssSPTb was shown to increase SPT activity and to modulate the acyl-CoA preference of SPT. In our analysis, we observed an increased canonical activity for three mutants (SPTLC1p.S331F, p.S331Y and SPTLC2p.I504F). Strikingly, the orthologous mutations in yeast were reported earlier to compensate for Tsc3 deficiency. In 2002, Monaghan *et al.* (53) found that the yeast mutant LCB1 p.I491F (the orthologue of SPTLC2p.I504F) can compensate for the lack of Tsc3. Han and co-workers (54) showed that the activation of SPT by the small subunits was altered for certain SPTLC2 mutations and that co-expressing the SPTLC1p.S331F mutant with SPTLC2 enabled a yeast SPT knockout strain to grow without the need for additional activation by ssSPTa. This suggests that these mutations influence the interaction of SPT with regulatory subunits such as ssSPTa and b. Accordingly, we found that canonical activity as well as 1-deoxy- and C_{20}SL formation increased in cells expressing SPTLC1p.S331F/Y or SPTLC2p.I504F mutants. Interestingly, both the residues SPTLC1p.S331 and SPTLC2p.I504 are located on the surface of the protein (Fig. 4A), suggesting that the apparent dysregulation of these mutants could be due to an impaired interaction with the small subunits ssSPTa or ssSPTb. A recently published paper reported that a mutation in ssSPTb is associated with increased C_{20}SL production and neurodegeneration in mice (55).

Clinical symptoms of patients carrying the SPTLC1p.S331F/Y or SPTLC2p.I504F mutation are clearly distinct from other HSAN1 cases. These variants are characterized by an early or congenital onset of symptoms, severe muscular impairments, growth retardation, early cataracts and impairments of the respiratory system (17,38). Motor neurons seem to be more dominantly affected in these patients compared with carriers of milder HSAN1 mutations who predominantly have sensory symptoms. We assume that the distinct clinical symptoms are directly related to the biochemical features in these mutants, although the mechanism by which they affect disease pathology remains to be determined. It is feasible that increased ceramide formation in cells expressing these variants causes, in addition to elevated 1-deoxySLs, further neurotoxic insults. However, total C_{18} SL levels were not elevated in the plasma of these patients, although this does not exclude that ceramide levels could be elevated in certain cells and tissues, including peripheral neurons or Schwann cells. Unfortunately, no biopsy material from these patients was available for comparison of ceramide levels between tissues.

The pathological formation of 1-deoxySLs is a hallmark of HSAN1, and plasma 1-deoxySL levels correlate significantly with disease severity (56). The HSAN1 mutations SPTLC1p.C133W, p.C133Y and also the recently found SPTLC2 mutations p.A182P, p.G382V and p.S384F are robustly associated with an increased 1-deoxySL formation, whereas mutations found in a non-HSAN1 context (such as the SPTLC1p.R151L or p.G382V) do not form 1-deoxySLs.

Although most analysed HSAN1 mutants coincided with this observation, there is one exception, which is the SPTLC1p.V144D mutant. In cell culture, the p.V144D showed no significant 1-deoxySL formation. However, the p.V144D mutation was one of the first two annotated HSAN1 mutations, and patients bearing this mutation present with elevated 1-deoxySL plasma levels and a HSAN1 phenotype. The reason for this discrepancy is not clear but indicates that additional, not yet characterized, systemic factors could influence 1-deoxySL formation, which might not be fully recapitulated in the cell-based assays. Independent of the type of mutation, 1-deoxySL formation was greatly reduced at elevated serine levels (Fig. 2G). In contrast, 1-dexoySL formation was significantly increased at elevated alanine levels. This indicates that L-serine supplementation could be a potential treatment for any form of HSAN1, irrespective of the underlying mutations.

In conclusion, we showed that mutations in SPT are functionally heterogeneous. Three different biochemical phenotypes are directly associated with three different clinical presentations: no HSAN1, late-onset and moderate HSAN1 or early onset and severe HSAN1. A more detailed understanding of the underlying structure–function–phenotype relationships is necessary to link these biochemical differences to the underlying pathomechanisms (57).

Materials and Methods

Ethical approval

Ethical approval for the here-used patient data was obtained by the respective local Institutional Review Boards. Written informed consent was obtained from all patients.

Generation of SPT mutants

Human SPTLC1 or SPTLC2 was cloned into pcDNA™3.1/V5-His (58) and modified by site-directed mutagenesis as described earlier (20). To generate the mutants, the following primer pairs were used:

SPTLC1_C133W_fw 5′-ggggacccagaggattttatggcacatttgatgttc-3′ SPTLC1_C133W_rv 5′-aggtacccacgcca tacttctttagagatgc taaagc-3′ SPTLC1_C133Y_fw 5′-atggtcctcgaggattttatggcaca tttgatgttc-3′ SPTLC1_C133Y_rv 5′-aggtacccacgcca tacttcttta gagatgctaaagc-3′ SPTLC1_V144D_fw 5′-gtggacccagaggatttta tggcacatttgatgatcatttggatttggaagaccg-3′ SPTLC1_V144D_ rv5′-aggtacccacgcca tacttctttagagatgctaaagc-3′ SPTLC1_ R151L_fW 5′-Ttcatttggatttggaagacctcctggcaaaatttatgaagac-

3′ SPTLC1_R151L_rv 5′-Gtcttcataaattttgccaggaggtcttccaaatccaaatgaa-3′ SPTLC1_R239W_fW 5′-Cctcgcaaggctcgtgtaacttggcgtttcatt-3′ SPTLC1_R239W_rv 5′-Aatgaaacgccaagttacacgagccttgcgagg-3′ SPTLC1_G246R_fW 5′-Cggcgtttcattgtagtagaacgattgtatatgaatactggaa-3′ SPTLC1_G246R_rv 5′-Ttccagtattcatatacaatcgttctactacaatgaaacgccg-3′ SPTLC1_S331F_fW 5′-Tgtaattgaccatcagcgacttttcggccagggata-3′ SPTLC1_S331F_rv 5′-Tatccctggccgaaaagtcgctgatggtcaattaca-3′ SPTLC1_S331Y_fW 5′-Tgtaattgaccatcagcgactttacggccagggata-3′ SPTLC1_S331Y_rv 5′-tatccctggccgtaaagtcgctgatggtcaattaca-3′ SPTLC1_A339V_fw 5′-gggatacTGCTTTTCAGtaagcTTACCTcccctgttagc-3′ SPTLC1_A339V_rv 5′-gctaacaggggAGGTAAgcttaCTGAAAAGCAgtatccc-3′ SPTLC1_A352V_fW 5′-Tgctgcagcaattgaggtcctcaacatcatggaag-3′ SPTLC1_A352V_rV 5′-Cttccatgatgttgaggacctcaattgctgcagca-3′ SPTLC1_G387A_FW 5′-aagtggtggcggagtccctttctccagccttt cacct-3′ SPTLC1_G387A_rv 5′-ttaatccagatatcccttgtaaagctttat gaatttgtcc-3′ SPTLC2_A182P_fw 5′-CAACTATCTTGGATTTCCCCGGAATACTGGATCATG-3′ SPTLC2_A182P_rv 5′-CATGATCCAGTATTCCGGGGAAATCCAAGATAGTTG-3′ SPTLC2_V359M_fW 5′-Ccacaggccggggtatggtggagtac-3′ SPTLC2_V359M_rv 5′-Gtactccaccataccccggcctgtgg-3′ SPTLC2_G382V_fW 5′-Gaacgttcacaaagagttttgttgcttctggaggatatattgg-3′ SPTLC2_G382V_rv 5′-Ccaatatatcctccagaagcaacaaaactctttgtgaacgttc-3′ SPTLC2_S384F_fw 5′-CAAAGAGTTTTGGTGCTTTCGGAGGATATATTGGAGGC-3′ SPTLC2_S384F_rv 5′-GCCTCCAATATATCCTCCGAAAGCACCAAAACTCTTTG-3′ SPTLC2_T409M_fW 5′-Tagtgcagtgtatgccatgtcattgtcacctcctg-3′ SPTLC2_T409M_rV 5′-Caggaggtgacaatgacatggcatacactgcacta-3′ SPTLC2_I504F_fW 5′-Ttcctgccacccc aatttttgagtccagagcc-3′ SPTLC2_I504F_rV 5′-Ggctctggactcaaaaattggggtggcaggaa-3′

All mutants and constructs were confirmed by sequencing.

Cell culture

HEK293 cells were cultured (37°C with 5% CO_2) in Dulbecco's modified Eagle's medium (DMEM) (Sigma), with 10% fetal calf serum (FCS) (Fisher Scientific FSA15-043), penicillin/streptomycin (100 U per ml/0.1 mg per ml, Sigma) and 400 μg/l G418 (Gibco). For storage, 5% of dimethyl sulfoxide (Sigma) was added and cells were frozen in $N_{2\ liq}$.

Transfection and expression

HEK293 cells (freshly obtained from the ATCC) were grown in six-well dishes up to 80% confluence and transfected with Lipofectamine 2000 (Life Technologies), according to the provided standard protocol. After 2 days, cells were transferred to selection medium containing P/S and 400 μg/l G418 (Gibco) and passaged a minimum of three times to establish stable cell lines.

Expression of the transfected plasmids was confirmed by western blot using a combination of His- and V5-tag antibodies (Serotec).

Metabolic labelling

About 250 000 cells/well were seeded in 2 ml fresh medium in six-well plates (BD Falcon) and cultured for 2 days to reach ~70–80% confluence. The medium was exchanged for L-serine- and L-alanine-free DMEM (Genaxxon Bioscience, Ulm, Germany), containing 10% FCS, P/S and 400 μg/ml G418. Two hours after medium exchange, isotope-labelled d3-N^{15}-L-serine (1 mm) and (2,3,3,3)-d4-L-alanine (2 mM) was added. In certain cases, Fumonisin B1 (FB1; 10 mg/ml in 100% EtOH) was also added to the cells (final concentration 35 μM). After 24 h, cells were harvested in 1 ml cold phosphate-buffered saline (PBS), counted (Beckman Coulter Z2), pelleted at 800 RCF at 4°C and stored at −20°C until further processing.

Lipid extraction

Sphingoid bases in cells were analysed from frozen cell pellets (2–3 million cells) re-suspended in 100 μl PBS or directly from human EDTA plasma (100 μl). Proteins were precipitated by adding 500 μl MeOH (Honeywell), including 200 pmol internal standards (d7-SA and d7-SO, Avanti Polar Lipids, Alabaster CA), and lipids were extracted under constant agitation (1 h, 1400 rpm at 37°C; Eppendorf Thermomixer Comfort; Eppendorf, Hamburg, Germany). Precipitated proteins were removed by centrifugation (5 min at 16 100 RCF, 22°C; Model 5415, Eppendorf), and the supernatant (500 μl) was transferred to a new tube, followed by the addition of 75 μl HCl (32%, Sigma). This mixture was incubated at 65°C for 16 h and finally neutralized by the addition of 100 μl KOH (10 M). Hydrolysed lipids were re-extracted by adding 125 μl $CHCl_3$, followed by the stepwise addition of another 500 μl $CHCl_3$, 100 μl NH_4OH [2N] and 500 μl alkaline H_2O. Samples were mixed thoroughly by vortexing between each step. Phases were separated by centrifugation at room temperature (13 000 g for 5 min). The upper phase was removed and the lower phase washed twice with alkaline H_2O (1 ml). The remaining $CHCl_3$ phase was evaporated under a flow of N_2 (Techne Sample Concentrator, Bibby Scientific Ltd, Staffordshire, UK), and lipids were stored under N_2 at −20°C.

Liquid chromatography–mass spectrometry (LC–MS)

For analysis, lipids were redissolved in 75 μl derivatization mix (56.7% MeOH, 33.3% EtOH and 10% H_2O) and derivatized with 5 μl of OPA working solution (990 μl boric acid [3%] + 10 μl *o*-phthalaldehyde [50 mg/ml in EtOH] + 0.5 μl 2-mercaptoethanol).

Samples were separated for 30 min on a reverse phase C18 column (Uptispere 120 Å, 5 μm, 125 mm × 2 mm, Interchim, France) with an isocratic mobile phase [1:1 methanol/ammonium acetate (5 mM; Sigma) in water] at a flow rate of 400 μl/min. After each run, the column was regenerated for 10 min with 100% MeOH.

Spectra were recorded on a triple quad MassSpec (TSQ Quantum Ultra, Thermo Scientific) in positive mode using APCI ionization.

Homology modelling and structural analysis

The human SPT model was generated using the homology-modelling server Swiss Model (http://swissmodel.expasy.org) (59–62). The subunits SPTLC1 and SPTLC2 were modelled separately based on the SPT structure from *Sphingomonas paucimobilis* (PBD code 2JG2). The resulting models showed QMEAN4 values of −9.89 and −6.50 and GMQE values of 0.63 and 0.55, respectively. The modelled SPTLC1 and SPTLC2 comprise residues D51 to I464 and T163 to G532, respectively. The dimer was built by aligning the modelled subunits onto the bacterial SPT (PBD code 2JGT) using Pymol.

Statistics

Statistical significance was calculated by one-way analysis of variance (ANOVA) and Dunnett's multiple comparison test using GraphPad Prism 5. The principal component analysis (PCA) was performed in SIMCA-P + (Umetrics).

Conflict of Interest statement. None declared.

Funding

The authors wish to thank the following funding sources for support: the 7th Framework Program of the European Commission ('RESOLVE', project no. 305707), the Swiss National Foundation SNF (project no. 31003A_153390/1), the Hurka Foundation, the Novartis Foundation and the Rare Disease Initiative Zurich ('radiz', Clinical Research Priority Program for Rare Diseases, University of Zurich).

References

1. Dyck, P. J. (1993) Neuronal atrophy and degeneration predominantly affecting peripheral sensory and autonomic neurons. In Dyck, P.J., Thomas, K.P., Griffin, J.W., Low, P.A. and Poduslo, J.F. (eds), *Peripheral Neuropathy*, 3rd edn, Saunders, Philadelphia, pp. 1065–1093.
2. Edvardson, S., Cinnamon, Y., Jalas, C., Shaag, A., Maayan, C., Axelrod, F.B. and Elpeleg, O. (2012) Hereditary sensory autonomic neuropathy caused by a mutation in dystonin. *Ann. Neurol.*, **71**, 569–572.
3. Leipold, E., Liebmann, L., Korenke, G.C., Heinrich, T., Giesselmann, S., Baets, J., Ebbinghaus, M., Goral, R.O., Stödberg, T., Hennings, J.C. *et al.* (2013) A de novo gain-of-function mutation in SCN11A causes loss of pain perception. *Nat. Genet.*, **45**, 1399–1404.
4. Auer-Grumbach, M. (2008) Hereditary sensory neuropathy type I. *Orphanet. J. Rare Dis.*, **3**, 7–7.
5. Houlden, H., King, R., Blake, J. and Groves, M. (2006) Clinical, pathological and genetic characterization of hereditary sensory and autonomic neuropathy type 1 (HSAN I). *Brain*, **1**, 411–425.
6. Denny-Brown, D.E. (1951) Hereditary sensory radicular neuropathy. *J. Neurol. Neurosurg. Psychiatr.*, **14**, 237–252.
7. Bejaoui, K., Wu, C., Scheffler, M.D., Haan, G., Ashby, P., Wu, L., de Jong, P. and Brown, R.H. (2001) SPTLC1 is mutated in hereditary sensory neuropathy, type 1. *Nat. Genet.*, **27**, 261–262.
8. Dawkins, J.L., Hulme, D.J., Brahmbhatt, S.B., Auer-Grumbach, M. and Nicholson, G.A. (2001) Mutations in SPTLC1, encoding serine palmitoyltransferase, long chain base subunit-1, cause hereditary sensory neuropathy type I. *Nat. Genet.*, **27**, 309–312.
9. Rotthier, A., Auer-Grumbach, M., Janssens, K., Baets, J., Penno, A., Almeida-Souza, L., Van Hoof, K., Jacobs, A., De Vriendt, E., Schlotter-Weigel, B. *et al.* (2010) Mutations in the SPTLC2 subunit of serine palmitoyltransferase cause hereditary sensory and autonomic neuropathy type I. *Am. J. Hum. Genet.*, **87**, 513–522.
10. Guelly, C., Zhu, P.-P., Leonardis, L., Papić, L., Zidar, J., Schabhüttl, M., Strohmaier, H., Weis, J., Strom, T.M., Baets, J. *et al.* (2011) Targeted high-throughput sequencing identifies mutations in atlastin-1 as a cause of hereditary sensory neuropathy type I. *Am. J. Hum. Genet.*, **88**, 99–105.
11. Klein, C.J., Botuyan, M.V., Wu, Y., Ward, C.J., Nicholson, G.A., Hammans, S., Hojo, K., Yamanishi, H., Karpf, A.R., Wallace, D.C. *et al.* (2011) Mutations in DNMT1 cause hereditary sensory neuropathy with dementia and hearing loss. *Nat Genet.*, **43**, 595–600.
12. Verhoeven, K., De Jonghe, P., Coen, K., Verpoorten, N., Auer-Grumbach, M., Kwon, J.M., FitzPatrick, D., Schmedding, E., De Vriendt, E., Jacobs, A. *et al.* (2003) Mutations in the small GTP-ase late endosomal protein RAB7 cause Charcot–Marie–Tooth type 2B neuropathy. *Am. J. Hum. Genet.*, **72**, 722–727.
13. Kornak, U., Mademan, I., Schinke, M., Voigt, M., Krawitz, P., Hecht, J., Barvencik, F., Schinke, T., Giesselmann, S., Beil, F.T. *et al.* (2014) Sensory neuropathy with bone destruction due to a mutation in the membrane-shaping atlastin GTPase 3. *Brain*, **137**, 683–692.
14. Hanada, K. (2003) Serine palmitoyltransferase, a key enzyme of sphingolipid metabolism. *Biochim. Biophys. Acta*, **1632**, 16–30.
15. Hornemann, T., Wei, Y. and Eckardstein, A.V.O.N. (2007) Is the mammalian serine palmitoyltransferase a high-molecular-mass complex? *Biochem J.*, **405**, 157–164.
16. Nicholson, G.A., Dawkins, J.L., Blair, I.P., Kennerson, M.L., Gordon, M.J., Cherryson, A.K., Nash, J. and Bananis, T. (1996) The gene for hereditary sensory neuropathy type I (HSN-I) maps to chromosome 9q22.1–q22.3. *Nat. Genet.*, **13**, 101–104.
17. Auer-Grumbach, M., Bode, H., Pieber, T.R., Schabhüttl, M., Fischer, D., Seidl, R., Graf, E., Wieland, T., Schuh, R., Vacariu, G. *et al.* (2013) Mutations at Ser331 in the HSN type I gene SPTLC1 are associated with a distinct syndromic phenotype. *Eur. J. Med. Genet.*, **56**, 266–269.
18. Rautenstrauss, B., Neitzel, B., Muench, C., Haas, J. and Holinski-Feder, E. pp. 290 of 381–290 of 381.
19. Rotthier, A., Baets, J., De Vriendt, E., Jacobs, A., Auer-Grumbach, M., Lévy, N., Bonello-Palot, N., Kilic, S.S., Weis, J., Nascimento, A. *et al.* (2009) Genes for hereditary sensory and autonomic neuropathies: a genotype–phenotype correlation. *Brain: J. Neurol.*, **132**, 2699–2711.
20. Ernst, D., Murphy, S.M., Sathiyanadan, K., Wei, Y., Othman, A., Laura, M., Liu, Y.T., Penno, A., Blake, J., Donaghy, M. *et al.* (2015) Novel HSAN1 mutation in serine palmitoyltransferase resides at a putative phosphorylation site that is involved in regulating substrate specificity. *Neuromol. Med.*, **17**, 47–57.
21. Hornemann, T., Penno, A., Richard, S., Nicholson, G., van Dijk, F.S., Rotthier, A., Timmerman, V. and von Eckardstein, A. (2009) A systematic comparison of all mutations in hereditary sensory neuropathy type I (HSAN I) reveals that the G387A mutation is not disease associated. *Neurogenetics*, **10**, 135–143.
22. Verhoeven, K., Coen, K., De Vriendt, E., Jacobs, A., Van Gerwen, V., Smouts, I., Pou-Serradell, A., Martin, J.J., Timmerman, V. and De Jonghe, P. (2004) SPTLC1 mutation in twin sisters with hereditary sensory neuropathy type I. *Neurology*, **62**, 1001–1002.
23. Sjöblom, T., Jones, S., Wood, L.D., Parsons, D.W., Lin, J., Barber, T.D., Mandelker, D., Leary, R.J., Ptak, J., Silliman, N. *et al.* (2006) The consensus coding sequences of human breast and colorectal cancers. *Science*, **314**, 268–274.
24. Hanada, K. (1998) Mammalian cell mutants resistant to a sphingomyelin-directed cytolysin. Genetic and biochemical evidence for complex formation of the LCB1 protein with the LCB2 protein for serine palmitoyltransferase. *J. Biol. Chem.*, **273**, 33787–33794.
25. Momin, A.A., Park, H., Allegood, J.C., Leipelt, M., Kelly, S.L., Merrill, A.H. and Hanada, K. (2009) Characterization of mutant serine palmitoyltransferase 1 in LY-B cells. *Lipids*, **44**, 725–732.
26. Meggouh, F., Bienfait, H.M.E., Weterman, M.a.J., de Visser, M. and Baas, F. (2006) Charcot–Marie–Tooth disease due to a de novo mutation of the RAB7 gene. *Neurology*, **67**, 1476–1478.
27. Penno, A., Reilly, M.M., Houlden, H., Laurá, M., Rentsch, K., Niederkofler, V., Stoeckli, E.T., Nicholson, G., Eichler, F., Brown, R.H. *et al.* (2010) Hereditary sensory neuropathy type 1 is caused by the accumulation of two neurotoxic sphingolipids. *J. Biol. Chem.*, **285**, 11178–11187.

28. Eichler, F.S., Hornemann, T., McCampbell, A., Kuljis, D., Penno, A., Vardeh, D., Tamrazian, E., Garofalo, K., Lee, H.-J., Kini, L. *et al.* (2009) Overexpression of the wild-type SPT1 subunit lowers desoxysphingolipid levels and rescues the phenotype of HSAN1. *J. Neurosci.***29**, 14646–14651.
29. Zitomer, N.C., Mitchell, T., Voss, K.A., Bondy, G.S., Pruett, S.T., Garnier-Amblard, E.C., Liebeskind, L.S., Park, H., Wang, E., Sullards, M.C. *et al.* (2009) Ceramide synthase inhibition by fumonisin B1 causes accumulation of 1-deoxysphinganine: a novel category of bioactive 1-deoxysphingoid bases and 1-deoxydihydroceramides biosynthesized by mammalian cell lines and animals. *J. Biol. Chem.*, **284**, 4786–4795.
30. Cuadros, R., Montejo de Garcini, E., Wandosell, F., Faircloth, G., Fernández-Sousa, J.M. and Avila, J. (2000) The marine compound spisulosine, an inhibitor of cell proliferation, promotes the disassembly of actin stress fibers. *Cancer Lett.*, **152**, 23–29.
31. Salcedo, M., Cuevas, C., Alonso, J.L. and Otero, G. (2007) The marine sphingolipid-derived compound ES 285 triggers an atypical cell death pathway. *Apoptosis*, 395–409.
32. Sánchez, A.M., Malagarie-Cazenave, S., Olea, N., Vara, D., Cuevas, C. and Díaz-Laviada, I. (2008) Spisulosine (ES-285) induces prostate tumor PC-3 and LNCaP cell death by de novo synthesis of ceramide and PKCzeta activation. *Eur. J. Pharmacol.*, **584**, 237–245.
33. Baird, R.D., Kitzen, J., Clarke, P.A., Planting, A., Reade, S., Reid, A., Welsh, L., López Lázaro, L., de las Heras, B., Judson, I.R. *et al.* (2009) Phase I safety, pharmacokinetic, and pharmacogenomic trial of ES-285, a novel marine cytotoxic agent, administered to adult patients with advanced solid tumors. *Mol. Cancer Ther.*, **8**, 1430–1437.
34. Schöffski, P., Dumez, H., Ruijter, R., Miguel-Lillo, B., Soto-Matos, A., Alfaro, V. and Giaccone, G. (2011) Spisulosine (ES-285) given as a weekly three-hour intravenous infusion: results of a phase I dose-escalating study in patients with advanced solid malignancies. *Cancer Chemother. Pharmacol.*, **68**, 1397–1403.
35. Vilar, E., Grünwald, V., Schöffski, P., Singer, H., Salazar, R., Iglesias, J.L., Casado, E., Cullell-young, M., Baselga, J. and Tabernero, J. (2012) A phase I dose-escalating study of ES-285, a marine sphingolipid-derived compound, with repeat dose administration in patients with advanced solid tumors. *Invest. New Drugs*, **30**, 299–305.
36. Zuellig, R.A., Hornemann, T., Othman, A., Hehl, A.B., Bode, H., Güntert, T., Ogunshola, O.O., Saponara, E., Grabliauskaite, K., Jang, J.-H. *et al.* (2013) Deoxysphingolipids, a novel biomarker for type 2 diabetes, are cytotoxic for insulin-producing cells. *Diabetes*, 1–45.
37. Huehne, K., Zweier, C., Raab, K., Odent, S., Bonnaure-Mallet, M., Sixou, J.-L., Landrieu, P., Goizet, C., Sarlangue, J., Baumann, M. *et al.* (2008) Novel missense, insertion and deletion mutations in the neurotrophic tyrosine kinase receptor type 1 gene (NTRK1) associated with congenital insensitivity to pain with anhidrosis. *Neuromusc. Disord.*, **18**, 159–166.
38. Suh, B.C., Hong, Y.B., Nakhro, K., Nam, S.H., Chung, K.W. and Choi, B.-O. (2014) Early-onset severe hereditary sensory and autonomic neuropathy type 1 with S331F SPTLC1 mutation. *Mol. Med. Rep.*, **9**, 481–486.
39. Bejaoui, K., Uchida, Y., Yasuda, S., Ho, M., Nishijima, M., Brown, R.H., Holleran, W.M. and Hanada, K. (2002) Hereditary sensory neuropathy type 1 mutations confer dominant negative effects on serine palmitoyltransferase, critical for sphingolipid synthesis. *J. Clin. Invest.*, **110**, 1301–1308.
40. Gable, K., Han, G., Monaghan, E., Bacikova, D., Natarajan, M., Williams, R. and Dunn, T.M. (2002) Mutations in the yeast LCB1 and LCB2 genes, including those corresponding to the hereditary sensory neuropathy type I mutations, dominantly inactivate serine palmitoyltransferase. *J. Biol. Chem.*, **277**, 10194–10200.
41. McCampbell, A., Truong, D., Broom, D.C., Allchorne, A., Gable, K., Cutler, R.G., Mattson, M.P., Woolf, C.J., Frosch, M.P., Harmon, J.M. *et al.* (2005) Mutant SPTLC1 dominantly inhibits serine palmitoyltransferase activity *in vivo* and confers an age-dependent neuropathy. *Hum. Mol. Genet.*, **14**, 3507–3521.
42. Riley, R.T., Wang, E., Schroeder, J.J., Smith, E.R., Plattner, R.D., Abbas, H., Yoo, H.S. and Merrill, A.H. (1996) Evidence for disruption of sphingolipid metabolism as a contributing factor in the toxicity and carcinogenicity of fumonisins. *Nat. Toxins*, **4**, 3–15.
43. Garofalo, K., Penno, A. and Schmidt, B.P. (2011) Oral l-serine supplementation reduces production of neurotoxic deoxysphingolipids in mice and humans with hereditary sensory autonomic neuropathy type 1. *J. Clin. Invest.*, 14–16.
44. Murphy, S.M., Ernst, D., Wei, Y., Laurà, M., Liu, Y.-T., Polke, J., Blake, J., Winer, J., Houlden, H., Hornemann, T. *et al.* (2013) Hereditary sensory and autonomic neuropathy type 1 (HSANI) caused by a novel mutation in SPTLC2. *Neurology*, **80**, 2106–2111.
45. Rotthier, A., Penno, A., Rautenstrauss, B., Auer-Grumbach, M., Stettner, G.M., Asselbergh, B., Van Hoof, K., Sticht, H., Lévy, N., Timmerman, V. *et al.* (2011) Characterization of two mutations in the SPTLC1 subunit of serine palmitoyltransferase associated with hereditary sensory and autonomic neuropathy type I. *Hum. Mutat.*, **32**, E2211–E2225.
46. Dedov, V.N., Dedova, I.V., Merrill, A.H. and Nicholson, G.A. (2004) Activity of partially inhibited serine palmitoyltransferase is sufficient for normal sphingolipid metabolism and viability of HSN1 patient cells. *Biochim. Biophys. Acta*, **1688**, 168–175.
47. Gupta, S.D., Gable, K., Alexaki, A., Chandris, P., Proia, R.L., Dunn, T.M. and Harmon, J.M. (2015) Expression of the ORMDLS, modulators of serine palmitoyltransferase, is regulated by sphingolipids in mammalian cells. *J. Biol. Chem.*, **290**, 90–98.
48. Breslow, D.K., Collins, S.R., Bodenmiller, B., Aebersold, R., Simons, K., Shevchenko, A., Ejsing, C.S. and Weissman, J.S. (2010) Orm family proteins mediate sphingolipid homeostasis. *Nature*, **463**, 1048–1053.
49. Roelants, F.M., Breslow, D.K., Muir, A., Weissman, J.S. and Thorner, J. (2011) Protein kinase Ypk1 phosphorylates regulatory proteins Orm1 and Orm2 to control sphingolipid homeostasis in *Saccharomyces cerevisiae*. *Proc. Natl Acad. Sci. USA*, **108**, 19222–19227.
50. Hjelmqvist, L., Tuson, M., Marfany, G., Herrero, E., Balcells, S. and Gonzàlez-Duarte, R. (2002) ORMDL proteins are a conserved new family of endoplasmic reticulum membrane proteins. *Genome Biol.*, **3**, RESEARCH0027–RESEARCH0027.
51. Siow, D.L. and Wattenberg, B.W. (2012) Mammalian ORMDL proteins mediate the feedback response in ceramide biosynthesis. *J. Biol. Chem.*, **287**, 40198–40204.
52. Han, G., Gupta, S.D., Gable, K., Niranjanakumari, S., Moitra, P., Eichler, F., Brown, R.H., Harmon, J.M. and Dunn, T.M. (2009) Identification of small subunits of mammalian serine palmitoyltransferase that confer distinct acyl-CoA substrate specificities. *Proc. Natl Acad. Sci. USA*, **106**, 8186–8191.
53. Monaghan, E., Gable, K. and Dunn, T. (2002) Mutations in the Lcb2p subunit of serine palmitoyltransferase eliminate the requirement for the TSC3 gene in *Saccharomyces cerevisiae*. *Yeast*, **19**, 659–670.

54. Harmon, J.M., Bacikova, D., Gable, K., Gupta, S.D., Han, G., Sengupta, N., Somashekarappa, N. and Dunn, T.M. (2013) Topological and functional characterization of the ssSPTs, small activating subunits of serine palmitoyltransferase. *J. Biol. Chem.*, **288**, 10144–10153.
55. Zhao, L.H., Spassieva, S., Gable, K., Gupta, S.D., Shi, L.Y., Wang, J.P., Bielawski, J., Hicks, W.L., Krebs, M.P., Naggert, J. *et al.* (2015) Elevation of 20-carbon long chain bases due to a mutation in serine palmitoyltransferase small subunit b results in neurodegeneration. *Proc. Natl Acad. Sci. USA*, **112**, 12962–12967.
56. Laurá, M., Murphy, S.M., Hornemann, T., Bode, H., Polke, J., Blake, J., Houlden, H. and Reilly, M.M. (2012) P42 hereditary sensory neuropathy type 1: correlation of severity and plasma atypical deoxy-sphyngoid bases. *Neuromusc. Disord.*, **22**, S18–S18.
57. Ernst, D. (2013) Regulation of deoxy-sphingolipids and their role in disease. PhD Thesis.
58. Hornemann, T., Richard, S., Rütti, M.F., Wei, Y., von Eckardstein, A., Serine-palmitoyltransferase, M., Ru, M.F. and Eckardstein, A.V. (2006) Cloning and initial characterization of a new subunit for mammalian serine-palmitoyltransferase. *J. Biol. Chem.*, **281**, 37275–37281.
59. Arnold, K., Bordoli, L., Kopp, J. and Schwede, T. (2006) The SWISS-MODEL workspace: a web-based environment for protein structure homology modelling. *Bioinformatics*, **22**, 195–201.
60. Biasini, M., Bienert, S., Waterhouse, A., Arnold, K., Studer, G., Schmidt, T., Kiefer, F., Cassarino, T.G., Bertoni, M., Bordoli, L. *et al.* (2014) SWISS-MODEL: modelling protein tertiary and quaternary structure using evolutionary information. *Nucleic Acids Res.*, **42**, W252–W258.
61. Guex, N., Peitsch, M.C. and Schwede, T. (2009) Automated comparative protein structure modeling with SWISS-MODEL and Swiss-PdbViewer: a historical perspective. *Electrophoresis*, **30**(Suppl. 1), S162–S173.
62. Kiefer, F., Arnold, K., Kunzli, M., Bordoli, L. and Schwede, T. (2009) The SWISS-MODEL Repository and associated resources. *Nucleic Acids Res.*, **37**, D387–D392.
63. Bi, H., Gao, Y., Yao, S., Dong, M., Headley, A.P. and Yuan, Y. (2007) Hereditary sensory and autonomic neuropathy type I in a Chinese family: British C133W mutation exists in the Chinese. *Neuropathology*, **27**, 429–433.
64. Klein, C.J., Wu, Y., Kruckeberg, K.E., Hebbring, S.J., Anderson, S.A., Cunningham, J.M., Dyck, P.J., Klein, D.M., Thibodeau, S.N. and Dyck, P.J. (2005) SPTLC1 and RAB7 mutation analysis in dominantly inherited and idiopathic sensory neuropathies. *J Neurol Neurosurg Psychiatry*, **76**, 1022–1024.
65. Geraldes, R., de Carvalho, M., Santos-Bento, M. and Nicholson, G. (2004) Hereditary sensory neuropathy type 1 in a Portuguese family-electrodiagnostic and autonomic nervous system studies. *J Neurol Sci.*, **227**, 35–38.
66. Rautenstrauss, B., Neitzel, B., Muench, C., Haas, J., Holinski-Feder, E. and Abicht, A. (2009) Late onset hereditary sensory neuropathy type 1 (hsn1) caused by a novel p.c133r missense mutation in sptlc1. *Journal of Peripheral Nervous System*, **14**, 124–125.